

---

# Nearly automatic vessels segmentation using graph-based energy minimization

*Release 1.00*

M. Freiman<sup>1</sup>, J. Frank<sup>1</sup>, L. Weizman<sup>1</sup> E. Nammer<sup>2</sup>,  
O. Shilon<sup>2</sup>, L. Joskowicz<sup>1</sup> and J. Sosna<sup>3</sup>

July 16, 2009

<sup>1</sup>School of Engineering and Computer Science, The Hebrew University of Jerusalem, Israel

<sup>2</sup>Simbionix, Ltd. Israel

<sup>3</sup>Department of Radiology, Hadassah Hebrew University Medical Center, Israel

## Abstract

We present a nearly automatic tool for the accurate segmentation of vascular structures in volumetric CTA images. Its inputs are a start and an end seed points inside the vessel. The two-step graph-based energy minimization method starts by computing the weighted shortest path between the vessel seed endpoints based on local image and seed intensities and vessel path geometric characteristics. It then automatically defines a Vessel Region Of Interest (VROI) from the shortest path and the estimated vessel radius, and extracts the vessels boundaries by minimize the energy on a corresponding graph cut.

We evaluate our method within the 2009 MICCAI 3D Segmentation Challenge for Clinical Applications Workshop. Experimental results on the 46 carotid bifurcations from clinical CTAs, compared to ground-truth generated by averaging three manual annotations, yield an average symmetric surface distance of 0.83mm and a Dice similarity of 81.8%, with only three input seeds. These results indicates that our method is easy to use, produces accurate segmentations of vessels lumen, and is robust to intensity variations inside the vessels, radius changes, bifurcations, and nearby anatomical structures with similar intensity values.

**Keywords:** minimal path, graph-cut, vessel lumen segmentation, carotid bifurcation

## Contents

<b>1</b>	<b>Introduction</b>	<b>2</b>
<b>2</b>	<b>Method</b>	<b>3</b>
2.1	Weighted shortest path computation	3
2.2	Optimal vessel boundary segmentation	4
<b>3</b>	<b>Experimental results</b>	<b>6</b>
<b>4</b>	<b>Conclusions</b>	<b>7</b>

---

## 1 Introduction

Vascular structures segmentation and modeling from volumetric Computed Tomography Angiography (CTA) images play an increasingly important role in diagnostic and interventional radiology. The models are used to diagnose a variety of conditions, such as atherosclerosis, vascular trauma, and aneurysms, and to plan and execute endovascular surgeries, such as carotid, coronary, and cerebral angiographic procedures. The tasks include 3D visualization, quantitative measurements, pathologies characterization, access and implant preoperative planning, image-guided surgery, and patient-specific simulation, among others.

Vascular structures segmentation has turned out to be a very challenging task, even when a radio-opaque dye is injected to improve the image contrast. The key difficulties include the vessels intensity range overlap with other nearby anatomical structures, the intensity inhomogeneity within the vessels, the intra-patient vessels geometry and intensity variability, and the presence of pathologies such as aneurysms, calcifications, and tumors, and of various implants, such as stents and bypasses. Manual segmentation is tedious, time-consuming, error-prone, and user-dependent, and is thus impractical for routine clinical practice.

Interactive vessels segmentation methods should be simple, generic, robust, accurate, and intuitive to use, so that the treating physician can produce and correct a vasculature segmentation in a few minutes. Recently developed methods can be classified into three main categories: 1) region growing [1], 2) fast marching and level-sets [12], and; 3) tracking methods [9]. For a review of vascular segmentation methods see [5]. Most of these methods require extensive user interaction and the adjustment of non-intuitive parameters to produce the desired results, which difficult their clinical use.

A promising approach is the graph min-cut interactive segmentation method [2, 4]. The image is represented as a graph whose nodes are the image voxels and whose edges are the voxels immediate neighbors. Two additional terminal nodes, 'source' and 'target' represent the vessels and background classes and are connected to the voxel nodes. Edge weights between voxel nodes correspond to the gradient strengths between them. Edge weights between voxel and terminal nodes correspond to the probability that the voxel belongs to the vessels or to the background class. The graph min-cut classifies the voxel nodes that separate the vessels from the background. The advantages of this method are that it is generic and that it is nearly parameter-free. Its drawbacks are that it requires significant user interaction, that it requires fine-tuning the vessels intensity priors which are very variable for small vessels, that it does not incorporate vessels geometric information, and that it is computationally intensive and has extensive memory requirements.

Recent improvements to the graph min-cut interactive segmentation method address some of these drawbacks. Slabaugh and Unal [11] add an elliptical shape prior term to the edges cost function. Sinop and Grady [10] use a Laplacian pyramid to accelerate the segmentation and reduce the memory usage. Ning et al. [7] use graph-cut active contours based on prior object surface estimation to improve the segmentation. Rother et al [8] propose user-selected enclosing rectangular regions around the objects of interest to reduce the user interaction. While this is useful for extracting simple objects in 2D images of natural scenes, it is laborious for 3D images of complex vascular structures. A key drawback of all these methods is that their generic segmentation framework is often ill-suited for 3D vessels segmentation.

We have developed a nearly automatic tool for the effective segmentation of vascular structures from CTA images. It only requires a start and an end seed point inside the vessel. The two-step graph-based method is robust to intensity variations inside the vessels, radius changes, pathologies such as aneurysms or calcifications, and the presence of nearby anatomical structures with similar intensity values.

This algorithm was developed as part a set of automatic and interactive tools for fast and accurate of patient specific models of vascular structures for patient specific simulations of minimally invasive endovascular surgeries. Patient-specific simulations have the potential to significantly reduce the physicians' learning

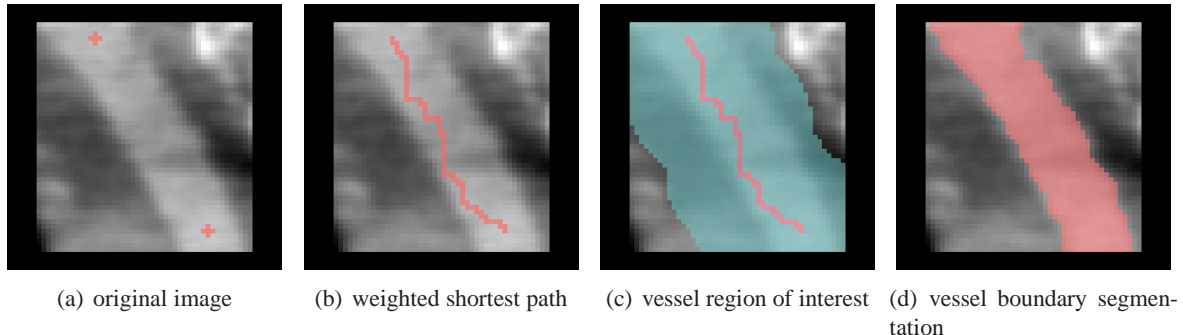


Figure 1: Illustration of the segmentation process on a clinical coronal CTA slice of the carotid artery: (a) detail of the original image showing the start and end vessel seed points (cross); (b) weighted shortest path between the two seeds; (c) vessel region of interest, and; (d) vessel boundary segmentation.

curve, reduce the outcome variability, and improve their performance. Existing training simulators such as the ANGIO Mentor™ (Simbionix Ltd, Israel) rely on hand-tailored anatomical models generated by a technician from CTA scans, which are impractical to produce patient-specific simulations in a clinical environment. Our segmentation tools produce accurate patient-specific models in a short time, thus making patient-specific simulations practical.

## 2 Method

Our interactive vessel boundary segmentation algorithm represents the image as a graph. It inputs a start and an end point of the vessel segment for which the boundary segmentation is required. The algorithm then proceeds in two steps: 1) weighted shortest path computation, and; 2) optimal vessel boundary segmentation. In the first step, it computes a path inside the vessel as the weighted shortest path between the graph nodes that contain the vessel endpoints. The edge weights compound local image and seed intensity information and vessel path geometric characteristics. In the second step, it constructs a Vessel Region of Interest (VROI) from the vessel path and the estimated vessel radius and computes the min-cut of the subgraph inside it. The min-cut identifies the graph nodes (voxels) at the boundary of the object (vessel) and background, thus producing the desired vessel boundary segmentation. Fig. 1 illustrates the method.

We describe each step in detail next. Let  $G = (V, E)$  be the image graph, where  $V = \{v_1, \dots, v_n\}$  are the graph nodes (one  $v_i$  per voxel) with their associated voxel intensity values  $I(v_i)$  and  $E = \{(v_i, v_j)\}$  are the graph edges, where  $v_i$  and  $v_j$  are neighboring voxels. Each node has 4 or 8 neighbors for 2D images, or 6 or 26 neighbors for 3D images. Each edge has a weight associated to it,  $w(v_i, v_j)$ . Graph nodes  $v_s$  and  $v_f$  are the user-defined start and end vessel seed points, and  $r$  is the estimated vessel radius.

### 2.1 Weighted shortest path computation

The vessel path is computed by finding the weighted shortest path between the vessel seed points  $v_s$  and  $v_f$  that is inside the vessel. The shortest path is the sequence of edges connecting  $v_s$  to  $v_f$  for which the sum of its edge weights is minimum. We use Dijkstra's shortest-path algorithm whose worst-case complexity is  $O(n^2)$ , where  $n$  is the number of voxels in the region of interest – initially all the image, but much smaller when the vessel seed points are nearby.

To robustly and accurately find the vessel path, we use a hybrid edge weighting function with intensity and geometric information. The edge weight is the sum of: 1) local intensity difference; 2) seed deviation intensity difference; 3) path smoothness; and 4) path length penalty.

The local intensity difference term is the squared difference of the edge voxel intensity values:

$$(I(v_i) - I(v_j))^2 \quad (1)$$

Since its value is large at boundary crossings, it prevents the path from leaving the vessel region.

The seed deviation intensity difference term is the sum of the relative squared differences of the seeds and edge end voxel intensity values:

$$(I(v_j) - I(v_s))^2 + (I(v_j) - I(v_t))^2 \quad (2)$$

This term prevents the edges in the path from diverging too much from the intensity values of the user-selected seed points. Its effect is to prevent the path to move along locally smooth tissues with low edge weights rather than moving inside the noisy vessel.

The path smoothness term is the angle between the edge voxels gradient directions:

$$|\cos^{-1}(\nabla v_i \cdot \nabla v_j)| \quad (3)$$

where  $\nabla$  is the normalized voxel gradient. This term prevents edges with large gradient differences to be added to the path.

The path length term is the Manhattan distance contribution of the edge. This term penalizes long paths, although when the path should not leave the vessel as it sometimes happens for highly curved vessels.

## 2.2 Optimal vessel boundary segmentation

The vessel boundary segmentation step starts by defining a Vessel Region of Interest (VROI) from the vessel path and the estimated vessel radius. It then updates the graph edge weights according to the VROI and computes the graph min-cut to identify vessel boundary voxels [7].

The VROI is computed as follows. First, two VROI boundaries are computed from each seed point by taking the perpendicular of the path at the seed point and symmetrically extending it by twice the estimated vessel radius. Within the band defined by the two line segments, all nodes that are at a distance of twice the estimated vessel radius from the vessel path are included in the VROI.

Next, the vessel boundary segmentation is formulated as a min-cut problem over the corresponding graph. We used the same graph representation as in the previous step, with additional two terminal nodes  $v_s, v_t$  correspond to object and background classes, respectively. In addition to the edges between voxels  $(v_i, v_j)$ , we add two edges for each voxel node  $v_i$ :  $(v_i, v_s), (v_i, v_t)$ . The edges  $(v_i, v_s)$  are from voxels to the object terminal node and the edges  $(v_i, v_t)$  are from voxels to the background terminal node.

Edge weights  $w(v_i, v_s)$  represent the probability that voxel  $v_i$  is related to the vessels or to the background:

$$w(v_i, v_s) = \exp\left(-\frac{I(v_i) - \mu_p}{\sigma_p}\right)^2 \cdot k \quad (4)$$

where  $\mu_p$  is the intensity mean value along the computed path,  $\sigma_p$  is the standard deviation and  $k$  is a scalar multiplier that depends on the distance between the current voxel  $v_i$  and the computed path. It represents the

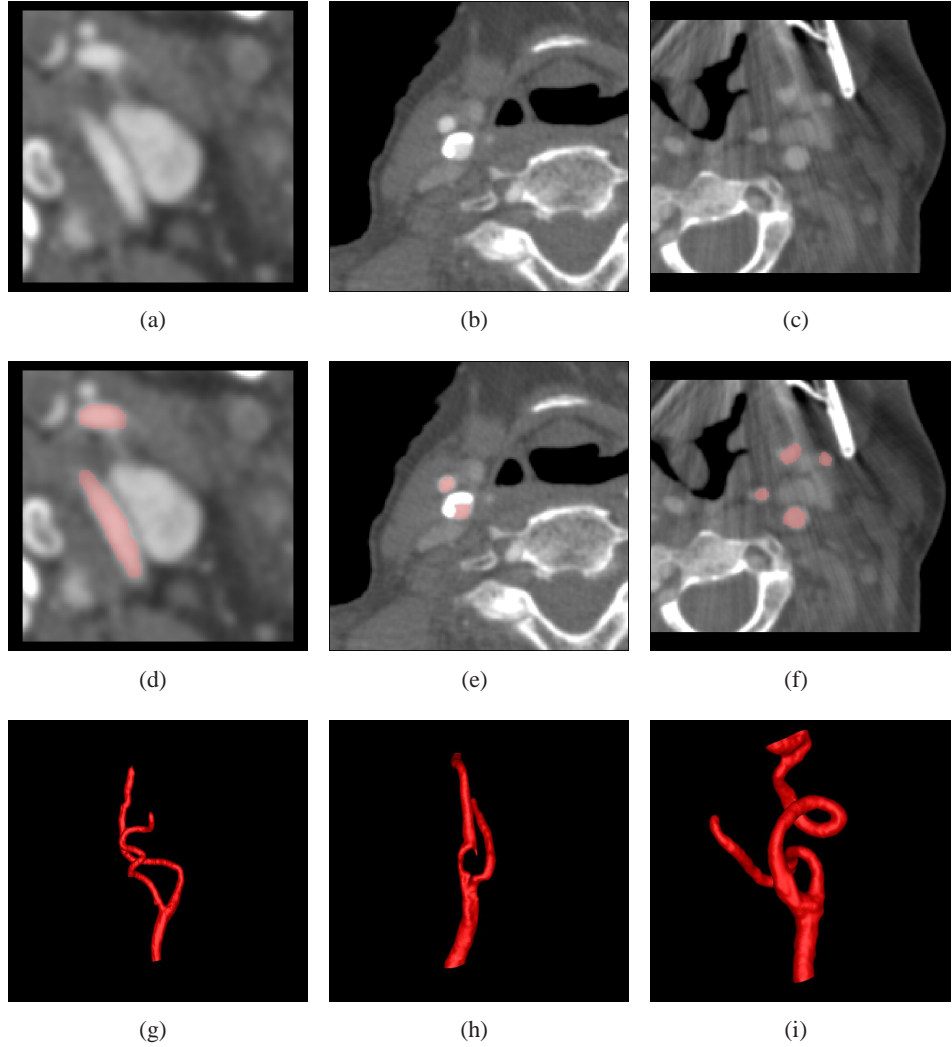


Figure 2: Carotid lumen segmentation results on several representative datasets: (a)-(c) original CTA images (d)-(f) 2D view of the segmentation results, overlaid on the original CTA slices. (g)-(i) 3D surface rendering of the results. 3D movies are available on: <http://www.cs.huji.ac.il/~freiman/vessels-cut>

probability that the voxel belongs to the object class based on voxel's intensity  $v_i$  and object's mean intensity value combined with spatial information that prefer voxels that are closer to the path computed before.

Edge weights  $w(v_i, v_t)$  represent the probability of each voxel to belong to background:

$$w(v_i, v_t) = 1 - w(v_i, v_s) \quad (5)$$

We use the inverse of the object weight  $w(v_i, v_s)$ , instead of explicit modeling of the background intensity,.

Edges weight  $w(v_i, v_j)$  represent the magnitude of the local gradient between the adjacent voxels:

$$w(v_i, v_j) = \exp \left( -\frac{I(v_i) - I(v_j)}{\sigma_p} \right)^2 \quad (6)$$

The optimal surface that separates the image into a vessel object and background is the min-cut at the resulting graph. The coupling of both intensity, gradients and path information yields an accurate vessel

Table 1: Summary lumen

Measure	% / mm			rank		
	min.	max.	avg.	min.	max.	avg.
L_dice	38.8%	94.3%	81.8%	3	4	3.97
L_msd	0.20mm	3.43mm	0.83mm	3	4	3.97
L_rmssd	0.35mm	5.82mm	1.54mm	4	4	4.00
L_max	1.02mm	16.67mm	5.98mm	3	4	3.97
<b>Total (lumen)</b>				<b>3</b>	<b>4</b>	<b>3.98</b>

Table 2: Averages lumen

Team name	Total success	dice		msd		rmssd		max		Total rank
		%	rank	mm	rank	mm	rank	mm	rank	
HUJI-CASMIP	31	81.8	4.0	0.83	4.0	1.54	4.0	5.98	4.0	4.0
Observer B	31	94.8	2.4	0.11	2.4	0.15	2.3	0.59	1.8	2.2
Observer C	31	94.7	2.2	0.11	2.2	0.15	2.1	0.71	2.4	2.2
Observer A	31	95.4	1.5	0.10	1.5	0.13	1.6	0.56	1.9	1.6

segmentation that accurately isolates even difficult regions such as bifurcations and pathologies including calcifications and aneurysms. Fig. 2 illustrates the method performance on pathological cases. Note that the resulting segmentation accurately separates the lumen from the calcifications, and segments the bifurcation.

### 3 Experimental results

We evaluated the performance of our method using the 3rd 3D segmentation challenge for clinical applications: carotid bifurcation algorithm evaluation framework [3], a MICCAI 2009 workshop. The datasets consists of 46 CTA images of the carotid arteries. For each image, three seed points were provided as input to the algorithm: one point on the Common Carotid Artery (CCA) 2cm below the carotid bifurcation. The second point is on the Internal Carotid Artery (ICA) 4cm cranial to the carotid bifurcation. The third point is on the External Carotid Artery (ECA) 2cm cranial to the carotid bifurcation. A detailed description of the datasets acquisition protocols and ground truth generation, can be found on [3]. From the 46 datasets, 14 were used for training, and the other 32 were used for the evaluation.

We compared our segmentation results to the ground-truth using five metrics: 1) Dice similarity measure; 2) Mean Symmetric absolute surface Distance (MSD); 3) Root Mean Square symmetric Surface Distance (RMSSD), and; 4) Maximum symmetric absolute surface distance.

Table 1 summarizes the results. The minimum, maximum, and average values for each metric are reported. Our method succeed in all cases to all the vasculatures defined in the ground-truth segmentation. The average Dice measure was 81.8% – in only in three cases the Dice similarity measure between our results and ground-truth was less than 70 (93.5% success rate) and in only 7 cases the Dice measure was less than 80 (85%). This success rate is much better than the previously reported success rate of 70% [6].

Table 2 shows the average grades of our method (HUJI-CASMIP) and of the three observers. The main reason that our method performance is worse than that of the observers is that our algorithm included small vascular structures that are not part of the ground truth, which consists of the CCA, the ICA and the ECA. The additional secondary branches and vessels segmented by our algorithm lowers the comparative grade (Fig. 3). The mean (std) computation time for each bifurcation was 2:02 (0:41) minutes using standard 3GHz PC with 4GB of memory.

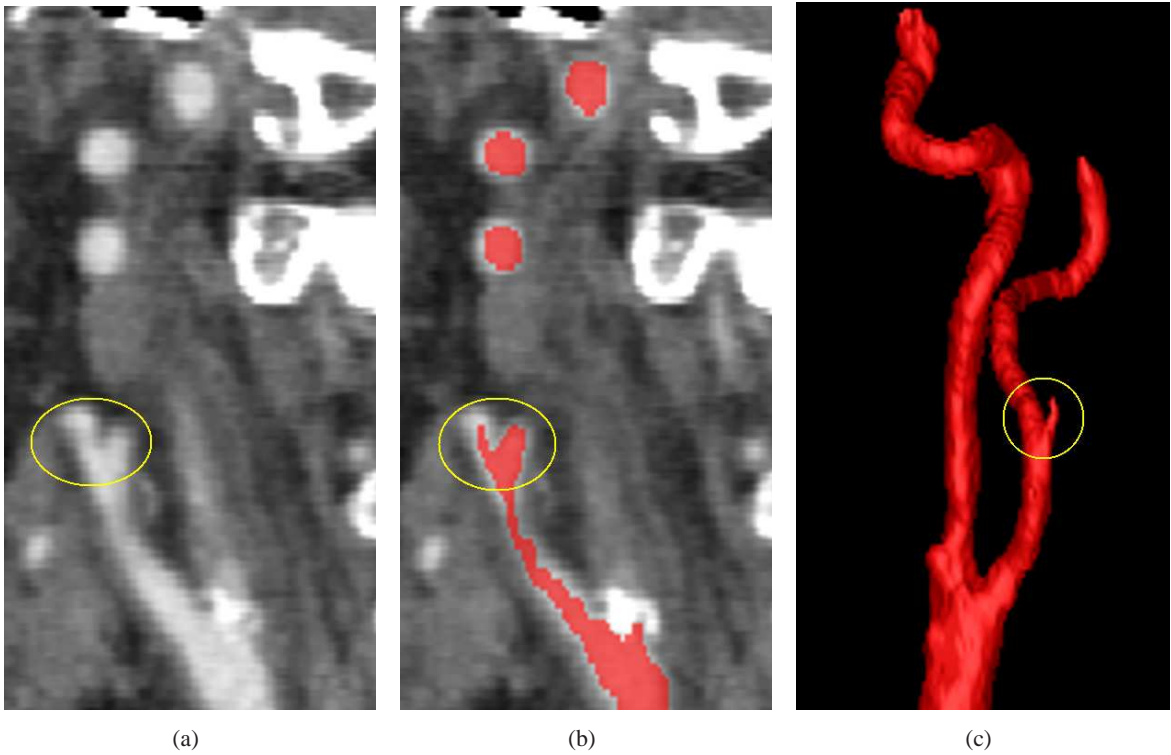


Figure 3: A small vessel branch from the ECA, encircled by a yellow ellipse, that segmented by our method, while do not consider as a vessel according to the ground truth.

## 4 Conclusions

We have presented an interactive tool for the accurate segmentation of vascular structures in volumetric CTA images. It inputs a start and an end seed points inside the vessel and an estimated vessel radius. The two-step graph-based method incorporates local image and seed intensities and vessel path geometric characteristics and automatically defines a Vessel Region Of Interest (VROI) in which a vessel path is computed.

The tool can be used to improve the results of other automatic segmentation methods, or on its own for the entire vessels segmentation. Our experimental results show that the tool is accurate, easy to use, robust to different initialization seeds, and can be applied for different vessels and imaging modalities.

## Acknowledgment

This research is supported in part by MAGNETON grant 38652 from the Israeli Ministry of Trade and Industry.

## References

- [1] S. Bock, C. Kühnel, T. Boskamp, and H.O. Peitgen. Robust vessel segmentation. In *Med. Imaging 2008: Computer-Aided Diagnosis*, volume 6915. SPIE, 2008. [1](#)
- [2] Y. Boykov and G. Funka-Lea. Graph cuts and efficient n-d image segmentation. *Int. J. of Comp. Vision*, 70(2):109–131, 2006. [1](#)
- [3] R. Hameeteman, M. Zuluaga, L. Joskowicz, M. Freiman, and T. van Walsum. 3D segmentation in the clinic: Carotid lumen segmentation and stenosis grading challenge. In R. Hameeteman, M. Zuluaga, L. Joskowicz, M. Freiman, and T. van Walsum, editors, *3D Segmentation in the Clinic: Carotid Lumen Segmentation and Stenosis Grading Challenge*, 2009. <http://cls2009.bigr.nl>. [3](#)
- [4] L. Kang, W. Xiaodong, D.Z. Chen, and M. Sonka. Optimal surface segmentation in volumetric images—a graph-theoretic approach. *IEEE Trans. Patt. Anal. and Mach. Intell.*, 28(1):119–134, 2006. [1](#)
- [5] C. Kirbas and F.K.H. Quek. A review of vessel extraction techniques and algorithms. *ACM Comput. Surv.*, 36(2):81–121, 2004. [1](#)
- [6] R. Manniesing, M.A. Viergever, and W.J. Niessen. Vessel axis tracking using topology constrained surface evolution. *IEEE Trans. Med. Imaging*, 26(3):309–316, 2007. [3](#)
- [7] X. Ning, A Narendra, and B. Ravi. Object segmentation using graph cuts based active contours. *Comp. Vision and Image Understanding*, 107(3):210–224, 2007. [1](#), [2.2](#)
- [8] C. Rother, V. Kolmogorov, and A. Blake. Grabcut: interactive foreground extraction using iterated graph cuts. *ACM Trans. Graph.*, 23(3):309–314, 2004. [1](#)
- [9] M. Schaap, R. Manniesing, I. Smal, T. Van Walsum, A. Van Der Lugt, and W.J. Niessen. Bayesian tracking of tubular structures and its application to carotid arteries in CTA. In *Proc. of the 10th Int. Conf. on Medi. Image Comp. and Comp. Aided Interventions, MICCAI'07*, volume 4792 of *LNCS*, pages 562–570, 2007. [1](#)
- [10] A.K. Sinop and L. Grady. Accurate banded graph cut segmentation of thin structures using laplacian pyramids. In *Proc. of the 9th Int. Conf. on Med. Image Comp. and Comp. Aided Interventions, MICCAI'06*, volume 4191 of *LNCS*, pages 896–903, 2006. [1](#)
- [11] G. Slabaugh and G. Unal. Graph cuts segmentation using an elliptical shape prior. In *Proc. of the 2005 IEEE Int. Conf. on Image Processing, ICIP'05*, volume 2, pages 1222–5, 2005. [1](#)
- [12] C.M. Van Bemmel, L.J. Spreeuwers, M.A. Viergever, and W.J. Niessen. Level-set based carotid artery segmentation for stenosis grading. In *Proc. of the 5th Int. Conf. on Medi. Image Comp. and Comp. Aided Interventions, MICCAI'02*, volume 2489 of *LNCS*, pages 36–43, 2002. [1](#)